FEM Model for Volume Fraction Dependent Interface Debonding in TiN Nanoparticle Reinforced AA7020 Metal Matrix Composites

[1]S. Sundara Rajan and A. Chennakesava Reddy[2]

[1]Scientist-F, Defence Research and Development Organisation, Hyderabad, India.
[2]Assistant Professor, Department of Mechanical Engineering, MJ College of Engineering and Technology, Hyderabad, India
dr_acreddy@yahoo.com

Abstract: A hexagonal array unit cell/2-D octahedron particulate RVE models were employed to predict interfacial debonding using cohesive zone method. The particulate metal matrix composites are TiN/AA7020 alloy at volume fractions of 10%, 20% and 30% TiN. The average particle size of TiN in composite was near 100 nm and it was well dispersed in octahedron shape. The cohesive zone analysis of interface debonding shows that the requirement of shear stress increases with increase of volume fraction of TiN for the occurrence of separation between nanoparticle and matrix.

Keywords: AA7020 alloy, titanium nitride, octahedron particle, RVE model, finite element analysis, interface debonding.

1. INTRODUCTION

Particulate metal matrix composites are being applied increasingly in structures due to their attractive characteristics like high stiffness-to-weight and strength-to-weight ratios. However, it is known that they are prone to develop internal damage, like matrix cracking and debonding, which can be particularly dangerous for structural stability leading to premature catastrophic failure. Consequently, the measurement of interfacial debonding becomes an important subject on these materials. The strength strongly depends on the stress transfer between the particles and the matrix. For well-bonded particles, the applied stress can be effectively transferred to the particles from the matrix [1]. The mechanical properties of particulate–polymer composites depend strongly on the particle size, particle–matrix interface adhesion and particle loading. A fundamental understanding of meta/ceramic interfaces has been elusive, despite their technological importance [2-15].

In this paper, cohesive zone method was applied to predict interfacial debonding in AA7020 alloy / titanium nitride nanocomposite. The compositions and micromechanics of AA7020/TiN nanocomposite were analyzed and characterized. Representative volume elements (RVEs) models were taken from the periodic 2-D octahedron particulates in a hexagonal array distribution (figure 1).

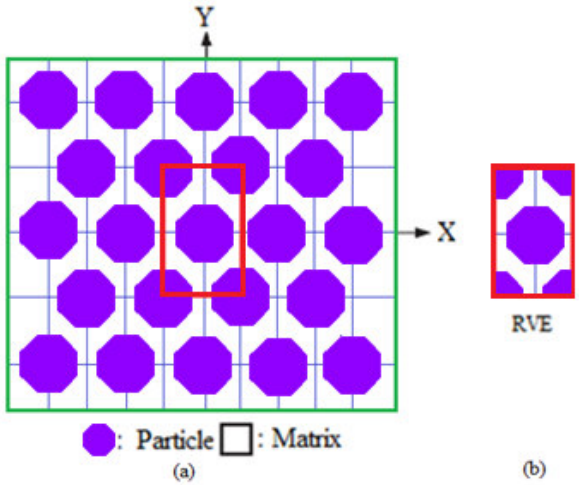

Figure 1: The RVE model.

2. MATERIALS AND METHODS

The volume fractions of TiN were chosen to be 10%, 20%, and 30% in the matrix of AA7020 alloy. Initially, both AA5050 and boron nitride were kept in contact along the interface in the x–y plane with zero separation distance. The simulation

domain is divided into three regions: Boron nitride nanoparticle, interface and AA505 alloy matrix. PLANE183 element was used for the matrix and the nanoparticulates. The cohesive element is implemented as a linear element with four nodes for the interface between TiN nanoparticle and AA7020 alloy matrix. Initially, the interface between the matrix material and the inclusion is assumed to be perfectly bonded. The finite element analysis was carried out for the single inclusion model undergoing a tensile load. The elastic material properties are given by E_m = 72.0 GPa, E_p = 251 GPa, ν_m = 0.33 and ν_p = 0.25.

Shear-log model is based on the assumption that all of the load transfer from matrix to particulate occurs via shear stresses acting on the particulate interface between the two constituents. The rate of change of the stress in the particulate to the interfacial shear stress at that point and the particulate radius, 'r' is given by:

$$\frac{d\sigma_p}{dx} = -\frac{2\tau_i}{r} \quad (1)$$

which may be regarded as the basic shear lag relationship.

The stress distribution in the particulate is determined by relating shear strains in the matrix around the particulate to the macroscopic strain of the composite. Some mathematical manipulation leads to a solution for the distribution of stress at a distance 'x' from the mid-point of the particulate which involves hyperbolic trig functions:

$$\sigma_p = E_p\varepsilon_c[1 - cosh(nx/r)sech(ns)] \quad (2)$$

where ε_c is the composite strain, s is the particulate aspect ratio (length/diameter) and n is a dimensionless constant given by:

$$n = \left[\frac{2E_m}{E_p(1+\nu_m)ln(1+\nu_p)}\right]^{1/2} \quad (3)$$

in which ν_m is the Poisson ratio of the matrix. The variation of interfacial shear stress along the particulate length is derived, according to Equation (1), by differentiating this equation, to give:

$$\tau_i = \frac{n\varepsilon_c}{2}E_p sinh\left(\frac{nx}{r}\right)sech(ns) \quad (4)$$

The equation for the stress in the particulate, together with the assumption of a average tensile strain in the matrix equal to that imposed on the composite, can be used to evaluate the composite stiffness. This leads to:

$$\sigma_c = \varepsilon_c\left[v_pE_p\left(1 - \frac{tanh(ns)}{ns}\right) + (1 - v_p)E_m\right] \quad (5)$$

The expression in square brackets is the composite stiffness. The stiffness is a function of particulate aspect ratio, particulate/matrix stiffness ratio and particulate volume fraction.

If the particle deforms in an elastic manner (according to Hooke's law) then,

$$\tau = \frac{n}{2}\sigma_p \quad (6)$$

If interfacial debonding/yielding is considered to occur when the interfacial shear stress reaches its shear strength

$$\tau = \tau_{max} \quad (7)$$

For particle/matrix interfacial fracture can be established whereby,

$$\tau_{max} < \frac{n\sigma_p}{2} \quad (8)$$

This approach suggests that the outcome of a matrix crack impinging on an embedded particle depends on the balance between the particle strength and the shear strength of the interface. For plane strain conditions, the macro stress- macro strain relation is as follows:

$$\begin{Bmatrix}\overline{\sigma_x}\\ \overline{\sigma_y}\\ \overline{\tau_{xy}}\end{Bmatrix} = \begin{bmatrix}\overline{C_{11}} & \overline{C_{12}} & 0\\ \overline{C_{21}} & \overline{C_{22}} & 0\\ 0 & 0 & \overline{C_{33}}\end{bmatrix} \times \begin{Bmatrix}\overline{\varepsilon_x}\\ \overline{\varepsilon_y}\\ \overline{\gamma_{xy}}\end{Bmatrix} \quad (9)$$

The interfacial tractions can be obtained by transforming the micro stresses at the interface as given in Eq. (3):

$$t = \begin{Bmatrix}t_z\\ t_n\\ t_t\end{Bmatrix} = T\sigma \quad (10)$$

where, $T = \begin{bmatrix}0 & 0 & 0\\ cos^2\theta & sin^2\theta & 2sin\theta cos\theta\\ -sin\theta cos\theta & sin\theta cos\theta & cos^2\theta - sin^2\theta\end{bmatrix}$

3. RESULTS AND DISCUSSION

The tensile and compressive moduli were nearly constant for three volume fractions of TiN as shown in figure 2a. The shear modulus increased with increase in the volume fraction of TiN in the composites (figure 2b). The major Poisson's ratio decreased with volume fraction of TiN. The stiffness mismatch between TiN nanoparticulate and AA7020 alloy matrix is 179

GPa. The condition $\tau_{max} < n\sigma_p/2$ is satisfied for the occurrence of debonding in the composites with 10%, 20% and 30% TiN (figure 3). The strain energy densities induced in the composites are shown in figure 4. The strain energy density is higher at the interface region around TiN nanoparticle than that for the matrix alloy and nanoparticle. The raster images obtained from the finite element analysis are shown in figure 5. The raster images indicate clearly the reduction strain energy at the interface due to separation of TiN nanoparticle from the AA7020 alloy matrix.

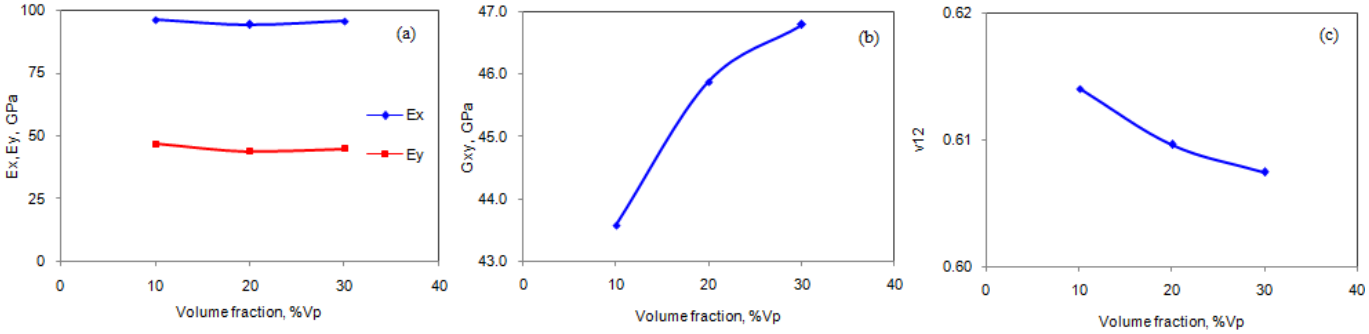

Figure 2: Effect of volume fraction on effective material properties.

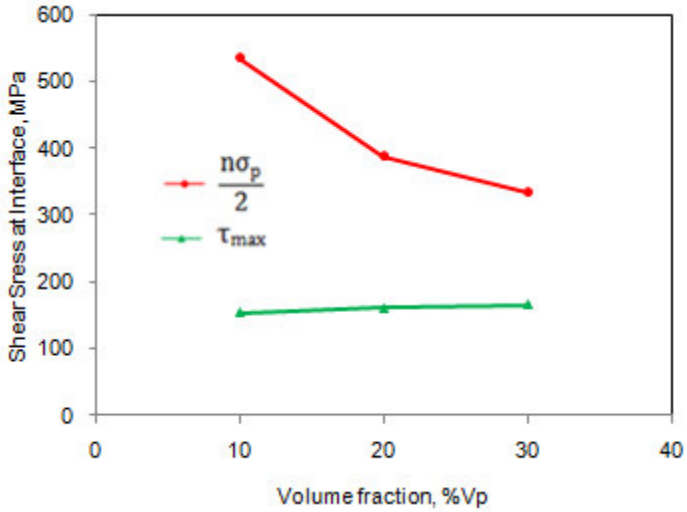

Figure 3: Fracture criteria of interface debonding.

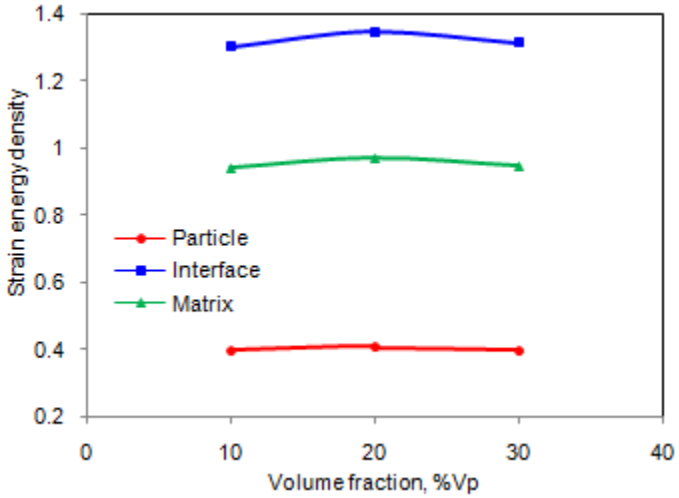

Figure 4: Effect of volume fraction on strain energy density.

The normal and tangential tractions are plotted in figure 6. Because of symmetry considerations, the variations of the interface stresses with circumferential location are plotted only for the range $0^o \leq \theta \leq 90^o$. The normal traction in the region of interface is high along the axis of tensile loading and it gradually reduced to zero at 71^o form axis of loading. The tangential traction becomes zero at an angle of 12^o from the axis of tensile loading. Even though, the separation begins at along the axis of tensile loading, it reaches progressively maximum at 71^o from the axis of loading along the interface. For the cause of interface debonding, the shear stress increased with increase of volume fraction of TiN in AA7020 alloy matrix.

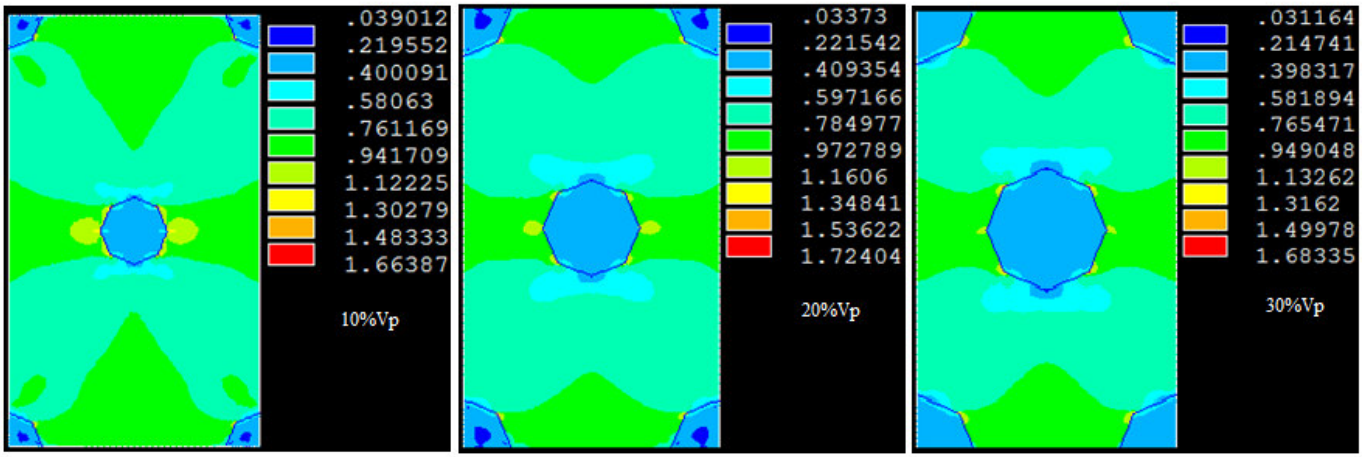

Figure 5: FEA results of strain energy densities.

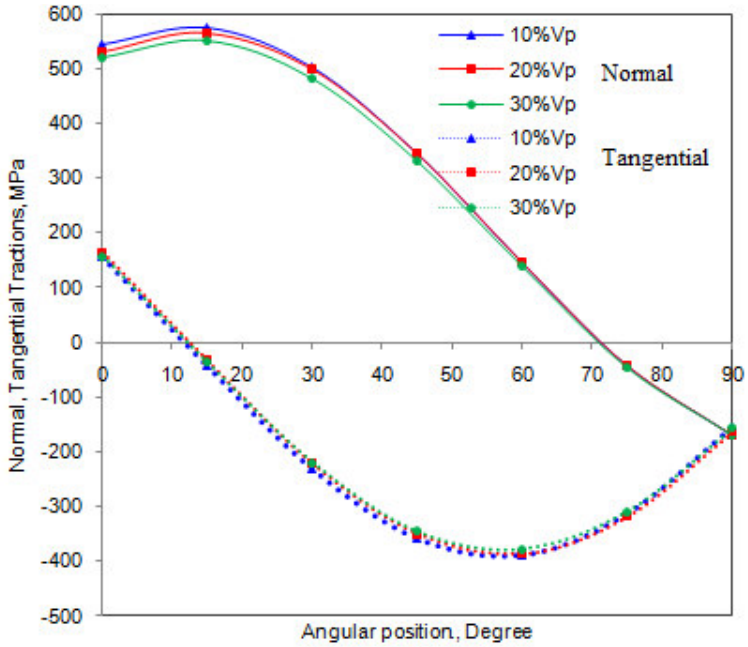

Figure 6: Normal and tangential: (a) tractions and (b) displacements.

4. CONCLUSION

The interface debonding occurred in the composites containing 10%, 20% and 30% volume fractions TiN. The shear stress increased with increase of volume fraction of TiN in AA7020 alloy matrix for the separation of nanoparticle from the matrix.

REFERENCES

1. C. H. Hsueh, Effects of aspect ratios of ellipsoidal inclusions on elastic stress transfer of ceramic composites, Journal of the American Ceramic Society, 72 1987, pp. 344–7.

2. A. Chennakesava Reddy, Assessment of Debonding and Particulate Fracture Occurrences in Circular Silicon Nitride Particulate/AA5050 Alloy Metal Matrix Composites , National Conference on Materials and Manufacturing Processes, Hyderabad, India, 27-28 February1998, pp.104-109.
3. B. Kotiveera Chari and A. Chennakesava Reddy, Numerical Simulation of Particulate Fracture in Round Silicon Nitride Particulate/AA6061 Alloy Metal Matrix Composites, National Conference on Materials and Manufacturing Processes, Hyderabad, India, 27-28 February 1998, pp. 110-114.
4. H. B. Niranjan and A. Chennakesava Reddy, Effect of Elastic Moduli Mismatch on Particulate Fracture in AA7020/Silicon Nitride Particulate Metal Matrix Composites , National Conference on Materials and Manufacturing Processes, Hyderabad, India, 27-28 February, 1998, pp. 115-118,
5. P. Martin Jebaraj and A. Chennakesava Reddy, Cohesive Zone Modelling for Interface Debonding in AA8090/Silicon Nitride Nanoparticulate Metal Matrix Composites, National Conference on Materials and Manufacturing Processes, Hyderabad, India, 27-28 February 1998, pp. 119-122.
6. P. Martin Jebaraj and A. Chennakesava Reddy, Plane Strain Finite Element Modeling for Interface Debonding in AA1100/Silicon Oxide Nanoparticulate Metal Matrix Composites, National Conference on Materials and Manufacturing Processes, Hyderabad, India, 27-28 February 1998, pp. 123-126.
7. A. Chennakesava Reddy, Local Stress Differential for Particulate Fracture in AA2024/Titanium Carbide Nanoparticulate Metal Matrix Composites, National Conference on Materials and Manufacturing Processes, Hyderabad, India, 27-28 February 1998, pp. 127-131.
8. B. Kotiveera Chari and A. Chennakesava Reddy, Interface Debonding and Particulate Facture based on Strain Energy Density in AA3003/MgO Nanoparticulate Metal Matrix Composites, National Conference on Materials and Manufacturing Processes, Hyderabad, India, 27-28 February 1998, pp. 132-136.
9. H. B. Niranjan and A. Chennakesava Reddy, Numerical and Analytical Prediction of Interface Debonding in AA4015/Boron Nitride Nanoparticulate Metal Matrix Composites , National Conference on Materials and Manufacturing Processes, Hyderabad, India, 27-28 February 1998, pp. 137-140.
10. S. Sundara Rajan and A. Chennakesava Reddy, Effect of Particulate Volume Fraction on Particulate Cracking in AA5050/Zirconium Oxide Nanoparticulate Metal Matrix Composites , National Conference on Materials and Manufacturing Processes, Hyderabad, India, 27-28 February 1998, pp. 156-159.
11. S. Sundara Rajan and A. Chennakesava Reddy, Cohesive Zone Analysis for Interface Debonding in AA6061/Titanium Nitride Nanoparticulate Metal Matrix Composites , National Conference on Materials and Manufacturing Processes, Hyderabad, India, 27-28 February 1998, pp. 160-164.
12. A. Chennakesava Reddy, Effect of Particle Loading on Microealstic Behavior and interfacial Tractions of Boron Carbide/AA4015 Alloy Metal Matrix Composites, 1st International Conference on Composite Materials and Characterization, Bangalore, 14-15 march 1997, pp. 176-179.7
13. A. Chennakesava Reddy, Reckoning of Micro-stresses and interfacial Tractions in Titanium Boride/AA2024 Alloy Metal Matrix Composites, 1st International Conference on Composite Materials and Characterization, Bangalore, 14-15 march 1997, pp. 195-197.
14. A. Chennakesava Reddy, Interfacial Debonding Analysis in Terms of Interfacial Tractions for Titanium Boride/AA3003 Alloy Metal Matrix Composites, 1st National Conference on Modern Materials and Manufacturing , Pune, India, 19-20 December 1997, pp. 124-127.
15. A. Chennakesava Reddy, Evaluation of Debonding and Dislocation Occurrences in Rhombus Silicon Nitride Particulate/AA4015 Alloy Metal Matrix Composites, 1st National Conference on Modern Materials and Manufacturing , Pune, India, 19-20 December 1997, pp. 278-282.